Communications in Physics, Vol. 33, No. 2 (2023), pp. 185-193
DOI: https://doi.org/10.15625/0868-3166/17445

Design and simulation of a thermal neutron beam for neutron capture studies at the Dalat research reactor

Trinh Thi Tu Anh[1,†], **Pham Dang Quyet**[1,‡], **Pham Ngoc Son**[2], **Phan Bao Quoc Hieu**[2], **Nguyen Thi Minh Sang**[1] **and Cao Dong Vu**[2]

[1] *1The University of Dalat, 01 Phu Dong Thien Vuong, Dalat, Lam Dong, Vietnam*
[2] *Nuclear Research Institute, 01 Nguyen Tu Luc, Dalat, Lam Dong, Vietnam*

E-mail: †anhttt@dlu.edu.vn; ‡quyetpd@dlu.edu.vn

Received 22 August 2022
Accepted for publication 14 February 2023
Published 23 April 2023

Abstract. *In this paper, a thermal neutron beam for neutron capture studies at the horizontal neutron channel No.2 of the Dalat Nuclear Research Reactor (DNRR) is designed and simulated using the MCNP5 code. The proposal model having a conical collimator of 240.3 cm in length, and neutron filters of Al_2O_3 and Bi crystals with different thicknesses was simulated for optimal adjustment of the filter lengths. The simulation shows that a pure thermal neutron beam can be obtained at the irradiation position when a composition of crystal filter of 20 cm Al_2O_3 and 6 cm Bi crystals are applied into the collimated beam line. The thermal and epithermal neutron fluxes are* 1.02×108 *n/cm^2/s (accounting for 97.92% of total neutron flux) and* 0.22×107 *n/cm^2/s (accounting for 2.08% of total neutron flux), respectively.*

Keywords: MCNP simulation; Al_2O_3 crystal; Bi crystal; thermal neutron flux.

Classification numbers: 28.41.Ak; 28.20.Ka; 28.20.Np.

1. Introduction

A thermal neutron beam of a nuclear reactor can be employed for neutron capture studies and applications such as prompt gamma neutron activation analysis (PGNAA), boron neutron capture therapy (BNCT) [1–6], and neutron radiography. To produce a thermal neutron beam from a nuclear reactor, single crystals of Si, Al_2O_3, or Bi are often used as neutron filters [5, 6]. A high-performance thermal neutron beam for neutron radiography using the Al_2O_3 sapphire crystal filter has been designed and developed at the PULSTAR reactor [7]. In our experimental studies of neutron capture reaction (n,γ), the activated nuclei with the exited state as its biding energy are considered to be produced. Accordingly, the thermal neutron beam with a high factor of thermal to fast neutron is required to reduce as most as possible unexpected reactions such as (n,p), (n,α), and (n,n').

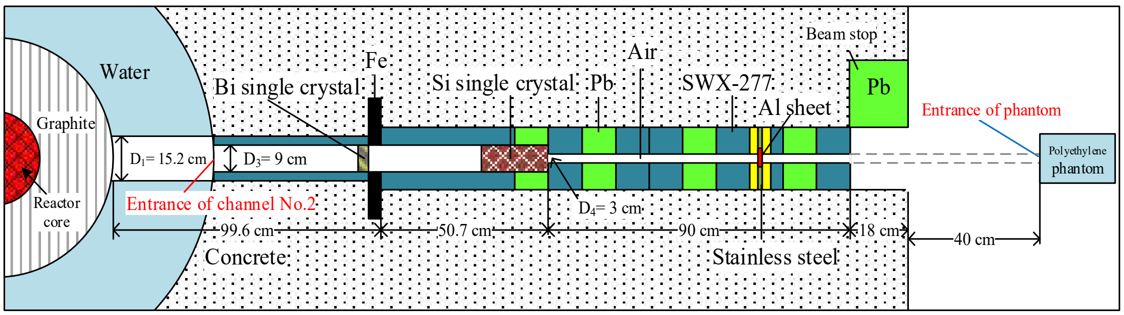

Fig. 1. The mechanical configuration of the horizontal channel No.2.

Fig. 2. MCNP5 Simulation model of the horizontal channel No.2.

In Vietnam, the Dalat nuclear research reactor (DNRR) is a 500-kW pool-type research reactor in which light water is used as both moderator and coolant, and the beryllium and graphite materials surrounding the reactor core are used as a neutron reflector [8]. The DNRR has four horizontal neutron channels that penetrate the concrete shield and the aluminum tank and pass through the pool water to the graphite reflector. Three of the neutron channels (No.1, No.2, and No.4) are oriented radially concerning the center of the reactor core, and channel No.3 is tangential to the outer edge of the reactor core [9]. The mechanical configuration and simulated figure of horizontal channel No.2 of the DNRR are presented in figures 1 and 2, respectively. From 2011 to the present, at the horizontal channel No. 2 of the DNRR, only a combination of Si and Bi single crystal filters has been used to provide a pure thermal neutron beam for different applications, such as PGNAA, nuclear data measurement, and training [8,9]. Therefore, this study aims to have a redesign and simulation check of the beam intensity and quality by replace the silicone filter material with the sapphire filters (Al_2O_3) at the horizontal neutron channel No.2 of the DNRR. We expect that the thermal neutron flux at the channel will improve significantly.

2. Materials and methods

The present configuration has a cylindrical collimator with a total length of 240.3 cm consisting of two parts. The first part is 150.3 cm in length and 9 cm in diameter for installing neutron filters made of Si and Bi crystals, with a thickness of 20 cm and 3 cm, respectively. The second part is 90 cm in length with an outer diameter of 20.1 cm, and the collimated diameter is 3 cm. The lining layers, surrounding the collimators, are made of Pb and WWX-277 (a neutron shielding material from the Shieldwerx company) as gamma and neutron absorbing materials and an aluminum plate for prevention from possible leaking water. The input neutron energy spectrum, for the simulation work was selected at the entrance position of the channel No.2, and validated by a gold foil activation method. The thermal and epithermal parts of the input spectrum are given in Fig. 3. The Bi crystal has the function of gamma-ray absorption, and the Si and Al_2O_3 crystals play the role of low transmission factors for fast neutrons but a high factor for thermal neutrons.

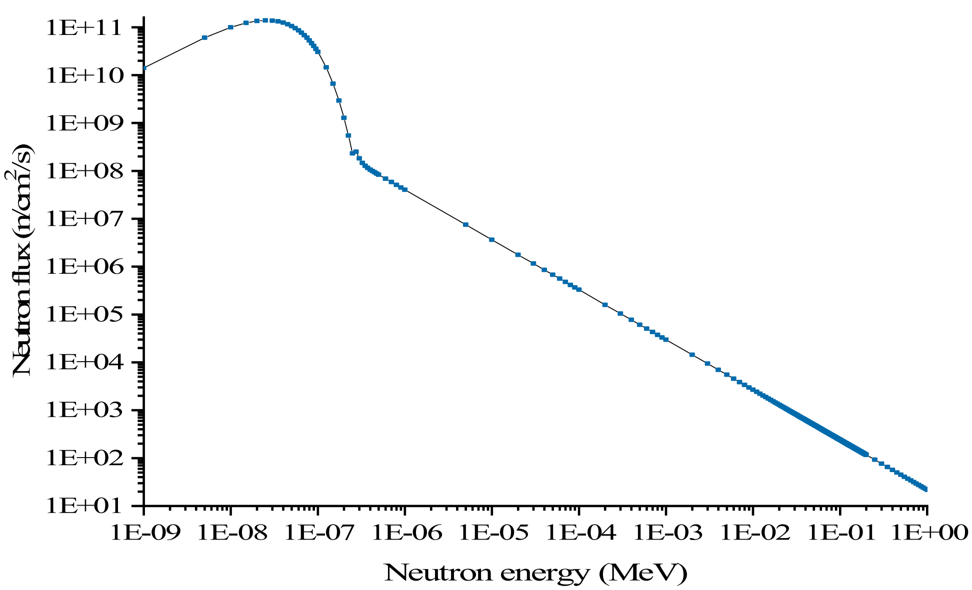

Fig. 3. The thermal and epithermal parts of the neutron energy spectrum at the entrance position of the channel No.2

The output neutron energy spectrum consisting of the thermal and epithermal neutron regions at the sample irradiation position after being transmitted through the filters was recorded using the tally F4 with DE4/DF4 cards of MCNP5 with an energy range from 1 meV upto 1 MeV.

The integrated thermal and epithermal fluxes were calculated from the output spectrum as follows [4, 10]:

$$\phi_{th} = \int_{1meV}^{E_{Cd}=0.5eV} \varphi_n(E)dE, \quad (1)$$

$$\phi_{epi} = \int_{E_{Cd}=0.5eV}^{100keV} \varphi_n(E)dE, \quad (2)$$

where ϕ is the neutron flux at the sample irradiation position, $\varphi_n(E)$ is the output energy dependent neutron, and E1 and E2 are the lower and upper limit of the energy range. In this work, the thermal neutron energy region covering the energy peak of 0.0253 eV was calculated from 1.0x10-3 eV to 0.5 eV, and the part from 0.5 eV to 0.1 MeV was considered as the epithermal neutron flux.

In this work, the neutron activation foils of vanadium with and without a Cd cover were irradiated at the output position for experimental determination of the thermal and epithermal neutron fluxes. The partial neutron flux can be calculated by the expression [11]:

$$\Phi = \frac{C \times f \times \lambda}{\varepsilon \times I \times N \times \sigma_0 \times \left(1 - e^{-\lambda t_1}\right) \times e^{-\lambda t_2} \times \left(1 - e^{-\lambda t_3}\right)}, \quad (3)$$

where Φ is the neutron flux, C the net counts of the corresponding gamma peak. f is the correction factor for the effects of neutron multiple scattering and self-shielding in the irradiated foils, λ is the decay constant of the ^{52}V product nucleus, and ε is the detection efficiency of the gamma-ray detector. I is the intensity of the gamma peak, N the number of ^{51}V nuclei in the foil sample, σ_0 is the average thermal neutron capture cross-section of ^{51}V. t_1, t_2, and t_3 are irradiating, cooling and measuring times, respectively. The uncertainties of the neutron fluxes presented in Table 1 are mainly from statistical and measured efficiency components.

Table 1. Simulated and measured results of the output thermal neutron flux at the channel No.2

Parameters	Simulation	Experimental
Thermal neutron flux ($n/cm^2/s$)	2.27×107	$(2.13 \pm 0.04) \times 107$

In this study, a conical collimator with 240.3 cm in length is proposed to increase neutron flux compared to a cylindrical collimator, presented in Ref. [5], which is used to simulate the neutron beam with the crystal filters of Al_2O_3 and Bi. This collimator model is presented in Fig. 4. The neutron total cross-sections of Al_2O_3 and Si crystal filters are prepared by using the NJOY16 code [12], as shown in Fig. 5. The cross section data base ENDF/B-VII.1 [13] has been updated in this MCNP5 simulations for the collimators materials.

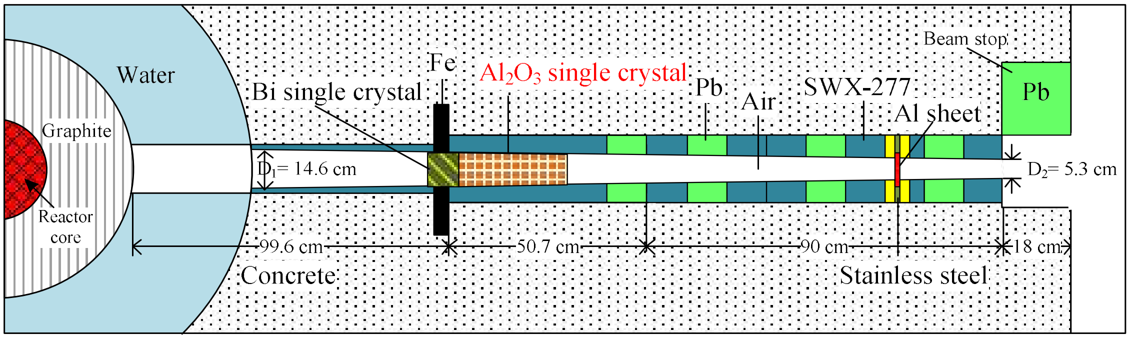

Fig. 4. The conical designing of collimators for the channel No.2 of the DNRR.

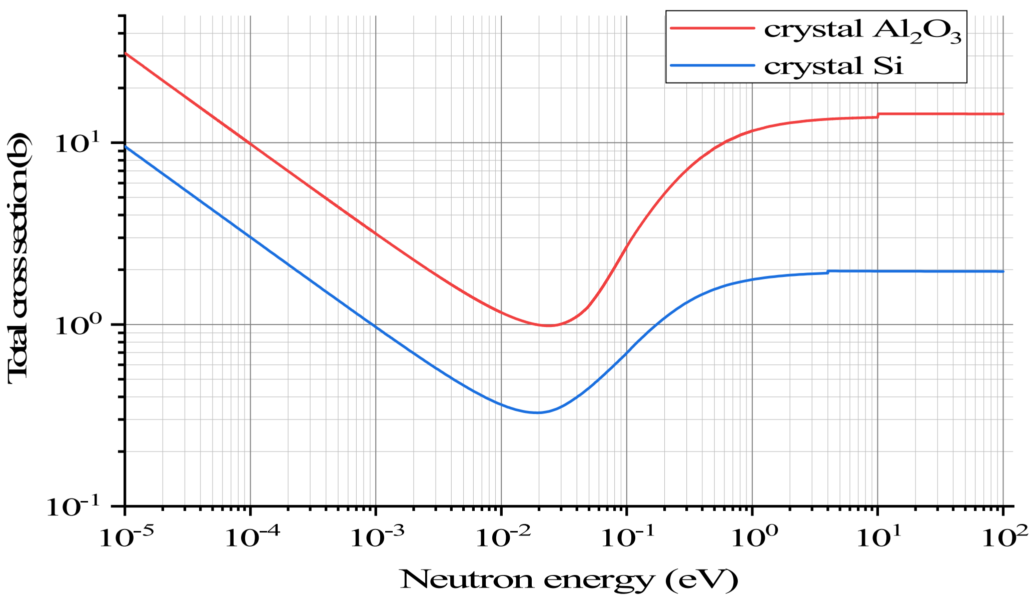

Fig. 5. Neutron total cross-section of Al_2O_3 and Si crystal filters.

3. Results and discussion

The thermal neutron fluxes at the sample irradiation position for cases of Al_2O_3 or Si crystal filters are determined by simulation. As shown in Fig. 6, the intensity of thermal neutron beam produced by the Al_2O_3 crystal filter is higher than that in the case of Si crystal filter. For the conical collimator model, the simulated values of the thermal and epithermal neutron fluxes at the sample irradiation position of the channel No.2 with alternative filter thickness are shown in the Table 2.

Filter thickness (cm)		Neutron flux					
		Thermal neutron 108 (n/cm^2/s)		Epithermal neutron 107 (n/cm^2/s)		Thermal/Total (%)	
Si/Al_2O_3	Bi	Si + Bi [5]	Al_2O_3 + Bi	Si + Bi [5]	Al_2O_3 + Bi	Si + Bi [5]	Al_2O_3 + Bi
0	0	4.68	4.68	16.92	16.92	73.43	73.43
5	1	3.46	3.38	8.49	4.49	80.30	88.28
5	2	2.95	2.89	6.58	3.5	81.79	89.19
5	3	2.53	2.48	5.12	2.75	83.17	90.01
5	4	2.18	2.15	3.99	2.16	84.53	90.88
5	5	1.88	1.85	3.04	1.71	86.10	91.55
5	6	1.63	1.61	2.36	1.36	87.33	92.20
10	1	3.02	2.89	5.51	1.89	84.56	93.85
10	2	2.58	2.48	4.27	1.51	85.77	94.26
10	3	2.21	2.13	3.32	1.2	86.96	94.66
10	4	1.91	1.84	2.59	0.96	88.09	95.05
10	5	1.64	1.59	1.97	0.8	89.31	95.25
10	6	1.42	1.38	1.52	0.63	90.36	95.63
15	1	2.64	2.48	3.65	0.89	87.84	96.55
15	2	2.26	2.13	2.87	0.72	88.74	96.75
15	3	1.94	1.83	2.19	0.58	89.86	96.94
15	4	1.67	1.59	1.74	0.47	90.58	97.13
15	5	1.44	1.38	1.35	0.41	91.42	97.12
15	6	1.25	1.20	1.01	0.32	92.50	97.37
20	1	2.32	2.15	2.42	0.55	90.57	97.52
20	2	1.99	1.84	1.91	0.45	91.24	97.60
20	3	1.74	1.58	1.46	0.37	92.24	97.73
20	4	1.47	1.37	1.12	0.3	92.89	97.84
20	5	1.26	1.18	0.90	0.27	93.36	97.73
20	6	1.09	1.03	0.73	0.22	93.72	97.92

It can be seen, in Table 2, that the thermal neutron fluxes by the Al_2O_3 crystal filter are slightly lower than the values by the Si crystal filter as the same thickness, but the quality factors (ratio of thermal neutron flux to epithermal neutron flux) of the neutron beam due to the Al_2O_3

filter is better. It can be explained based on Fig. 5, that neutron total cross-section in the energy range from 10^5 eV to 100 eV of the crystal Al_2O_3 is higher than Si crystal. In addition, in the epithermal neutron energy range from 0.5 eV to 100 eV, the neutron capture cross-section of the Al_2O_3 crystal is much higher than Si crystal, therefore the epithermal neutron flux at the irradiation position generated by crystal Al_2O_3 is much lower than crystal Si. In other words, we only need 25 cm of the crystal Al_2O_3 filter in length to produce the pure thermal neutron beam (98.40% of total neutron flux) with a value of 0.89×108 n/cm^2/s while the crystal Si filter is 60 cm in length (98.33% of total neutron flux) with the value of 0.40×108 n/cm^2/s, respectively.

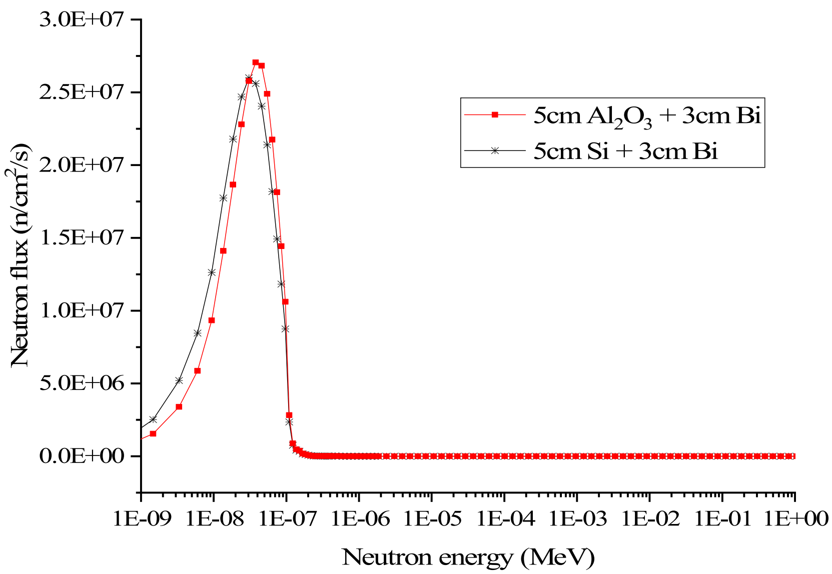

Fig. 6. The output neutron spectrum at the sample position by using Al_2O_3 and Si crystal filters.

As seen in Fig. 7, the thermal neutron flux decreases nun-uniformly with an increase of the same amount of thickness of the Bi filter. For every 5-cm Al_2O_3 added, its ability to reduce the thermal neutron flux is almost the same as that of an increase of 1 cm Bi. Fig. 7 also shows the effect on the thermal neutron flux as the thickness of the Al_2O_3 filter further increases. This effect is greatest with the second 5 cm Al_2O_3 (at 10 cm) and gradually less with each subsequent 5 cm.

Figure 8 and Table 2 indicate that the quality factors of the thermal neutron beam also increases non-uniformly as increasing the thickness of Al_2O_3 and Bi filters. The optimal thickness of Al_2O_3 crystal is 20 cm.

4. Conclusions

In order to to improvement of the thermal neutron beam of channel No. 2 for neutron capture experiment and related applications, the MCNP simulations of channel No.2 of the DNRR with different thicknesses of Al_2O_3 and Bi single crystal filters were carried out. The quality factors of the thermal neutron beam in the case of Al_2O_3 crystal is better than the previous ones (Si crystals). A composite of 20 cm Al_2O_3 and 6 cm Bi single crystals has proposed for the PGNAA

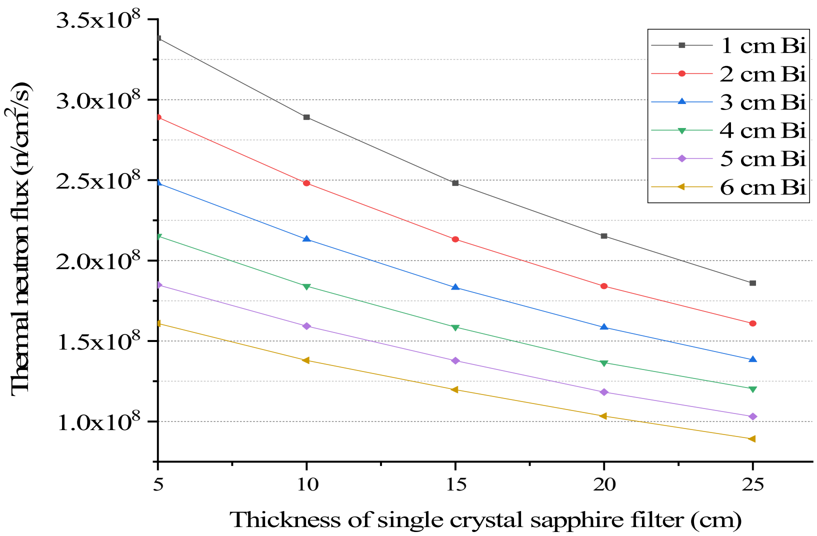

Fig. 7. Thermal neutron flux according to the length of the crystal filters of Al_2O_3 and Bi

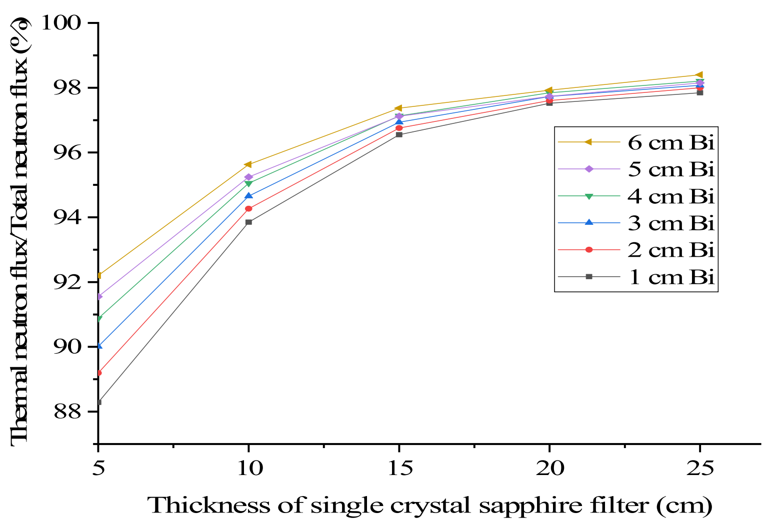

Fig. 8. Thermal neutron flux ratio according to the length of the crystal filters of Al_2O_3 and Bi

application that the thermal and epithermal neutron fluxes at the sample irradiation position would be 1.03×108 n/cm^2/s (97.92% of total neutron flux) and 0.22×107 n/cm^2/s (2.08% of total neutron flux), respectively. The simulated results of thermal neutron beams in this paper are also expected to be useful for basic experimental research and education using the neutron beam facilities at the DNRR.

Acknowledgements

This work has been carried out with the financial support of the Ministry of Science and Technology of Vietnam under a project encoded "B2021-DLA-02".

Conflict of interest

The authors have no conflicts of interest to declare.

References

[1] T. Matsumoto, *Design of neutron beams for boron neutron capture therapy for Triga reactor*, J. Nucl. Sci. Technol. **33** (1996) 171.

[2] M. Monshizadeh, Y. Kasesaz, H. Khalafi and S. Hamidi, *MCNP design of thermal and epithermal neutron beam for BNCT at the Isfahan MNSR*, Progress in Nuclear Energy **83** (2015) 427.

[3] J. Brockman, D. W. Nigg, M. F. Hawthorne and C. McKibben, *Spectral performance of a composite single-crystal filtered thermal neutron beam for BNCT research at the University of Missouri*, Appl. Radiat. Isotopes **67** (2009) 223.

[4] J. Byung-Jin and L. Byung-Chul, *A NCT facility design at HANARO*, in *Frontiers in Neutron Capture Therapy*, Plenum Publishers, New York, pp. 319-323, (2001).

[5] Pham Dang Quyet, Pham Ngoc Son, Nguyen Nhi Dien, Trinh Thi Tu Anh and Cao Dong Vu, *Simulation design of thermal neutron collimators for neutron capture studies at the Dalat Research Reactor*, Asian J. Sci. Res. **13** (2020) 214.

[6] K. Myong-Seop *et al.*, *Development and characteristics of the HANARO neutron irradiation facility for applications in the boron neutron capture therapy field*, Phys. Med. Biol. **52** (2007) 2553.

[7] K. Mishra, A. I. Hawari and V. H. Gillette, *Design and performance of a thermal neutron imaging facility at the North Carolina State university PULSTAR reactor*, IEEE Trans. Nucl. Sci. **56** (2006) 3904.

[8] Nguyen Nhi Dien *et al.*, *Utilisation of the Dalat Research Reactor after its core conversion*, in *Joint IGORR 2014/ IAEA Technical Meeting*, Bariloche, Argentina, 2014.

[9] Pham Ngoc Son, Vuong Huu Tan, Nguyen Nhi Dien, Nguyen Xuan Hai, Tran Tuan Anh, Ho Huu Thang and Cao Dong Vu, *Development of thermal filtered neutron beam based on the radial channel No. 2 of Dalat research reactor*, Science and Technics Publishing House, pp. 21-27, 2010.

[10] Y. Kasesaz *et al.*, *BNCT project at Tehran Research Reactor: current and prospective plans*, Progress in Nuclear Energy **91** (2016) 107.

[11] J. Abdelhamid, A. J. Hamid, C. Abdelouahed, K. Ouadie and S. Abdelmajid, *Generation of thermal scattering cross sections for Sapphire (Al_2O_3) and Bi Crystal filters used in nuclear facilities*, Physics AUC **29** (2019) 45.

[12] W. Haeck, J. L. Conlin, A. P. McCartney and A. C. III. Kahler, NJOY2016 updates for ENDF/B-VIII.0. United States: N. p., 2018.

[13] National Nuclear Data Center, *ENDF/B-VII.1 evaluated nuclear data library* [online], 2015. URL: http://www.nndc.bnl.gov/endf/b7.1/.